IEEE Photonics Journal
An IEEE Photonics Society Publication

Open Access

Fabrication of Low-Cost Multiwavelength Laser Arrays for OLTs in WDM-PONs by Combining the SAG and BIG Techniques

Volume 7, Number 4, August 2015

Liangshun Han
Song Liang
Huitao Wang
Junjie Xu
Lijun Qiao
Hongliang Zhu
Wei Wang

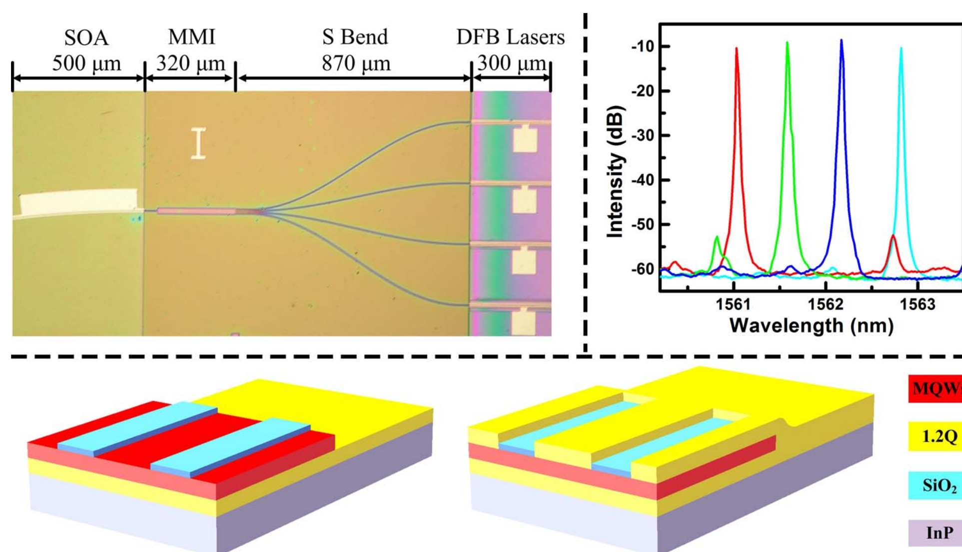

DOI: 10.1109/JPHOT.2015.2439957
1943-0655 © 2015 IEEE

IEEE photonics SOCIETY
IEEE

Fabrication of Low-Cost Multiwavelength Laser Arrays for OLTs in WDM-PONs by Combining the SAG and BIG Techniques

Liangshun Han, Song Liang, Huitao Wang, Junjie Xu, Lijun Qiao, Hongliang Zhu, and Wei Wang

Key Laboratory of Semiconductor Materials Science, Institute of Semiconductors, Chinese Academy of Sciences, Beijing 100083, China

DOI: 10.1109/JPHOT.2015.2439957
1943-0655 © 2015 IEEE. Translations and content mining are permitted for academic research only. Personal use is also permitted, but republication/redistribution requires IEEE permission. See http://www.ieee.org/publications_standards/publications/rights/index.html for more information.

Manuscript received April 28, 2015; revised May 23, 2015; accepted May 27, 2015. Date of publication June 1, 2015; date of current version July 7, 2015. This work was supported in part by the National "863" Project under Grant 2013AA014502 and Grant 2011AA010303; by the National Natural Science Foundation of China under Grant 61474112, Grant 61274071, Grant 61090392, and Grant 61006044; and by the National 973 Program under Grant 2012CB934202. Corresponding author: S. Liang (e-mail: liangsong@semi.ac.cn).

Abstract: We present the fabrication of a low-cost multiwavelength laser array monolithically integrated with a passive optical combiner for optical line terminals (OLTs) in wavelength-division multiplexing (WDM) passive optical networks (PONs). By combining the upper separate confinement heterostructure layer selective area growth technique and the bundle integrated guide technique, both multiwavelength emission with highly uniform spacing and low-loss passive-waveguide material can be obtained in a single metal–organic chemical vapor deposition (MOCVD) growth step, which greatly simplifies the fabrication of the device. A prototype laser array, which has four distributed feedback (DFB) laser elements and a multimode interference coupler as combiner, is successfully fabricated. The shallow ridge structure of the DFB lasers and the deep ridge structure of the passive waveguides are obtained by a single dry etching step, which further eases the device fabrication. The properties of the device are measured and discussed. The results indicate that our method is promising for fabricating cost-effective OLT light sources for WDM-PONs.

Index Terms: Integrated optics devices, laser arrays.

1. Introduction

Passive optical network (PON) is one of the most attractive optical access network schematics to meet the ever-increasing demand for high-bandwidth services such as internet protocol (IP) video delivery and voice-over IP (VoIP) because the infrastructures of PONs can be shared by many customers, making it highly cost-effective [1]. The capacity of PONs can be effectively extended by the introduction of wavelength division multiplexing (WDM) technique, forming the WDM-PONs, which are attracting great attention in recent years [2]. Up to now, a number of works of research on the realization of colorless transmitters of ONUs have been done to reduce the costs related to the inventory and management of the transmitters. Techniques that have been presented include reflective semiconductor optical amplifiers (RSOAs) [3], injection locked Fabry–Pérot (FP) laser diodes [4], and tunable lasers [5]. However, only a few studies on the development of cost-effective light sources used for optical line terminals (OLTs) have been reported [6]. It is obvious that high-quality transmitters of OLTs will also help in improving the performance of WDM-PONs.

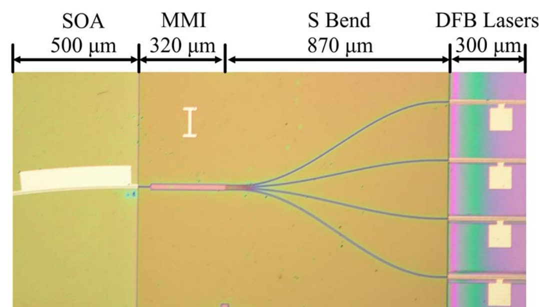

Fig. 1. Top view of the optical microscope image of the fabricated device.

Multi-wavelength distributed feedback (DFB) laser arrays are good candidates for OLT light sources. When compared with multiple discrete DFB lasers, laser arrays have many advantages such as lower packaging cost, lower power consumption, and compact size [7]–[9]. However, it is not easy to fabricate high-performance multi-wavelength laser arrays. First, different laser emissions, which are uniformly spaced, have to be defined side by side on the wafer. Electron beam lithography (EBL) is usually used to obtain different emission wavelengths, which is, however, an expensive and time-consuming technique [7]. Other techniques such as multi-quantum well (MQW) selective area growth (SAG) and ridge width variation were also used. For the MQW SAG technique, it is difficult to get uniform wavelength spacing because of the quality degradation of the MQW material induced by the SAG process [8]. Ridge variation may lead to multilateral modes [9]. Then, the emissions from different laser elements should be collected into a single waveguide before being coupled into a single mode fiber for transmission in PONs. In [6], a separate array waveguide grating (AWG) combiner is used. The disadvantage of the scheme is that a low coupling loss of light power between the laser waveguide and the AWG waveguide is hard to achieve. To get a high coupling efficiency, several techniques that can be used to monolithically integrate power combiner with the laser array have been developed. Typical techniques include the butt-joint technique and the quantum well intermixing (QWI) technique. The butt-joint technique needs an additional material growth step, which requires careful optimization of the growth conditions [10]. To obtain a large wavelength blue shift by the QWI process [11], it is more or less usually accompanied by deterioration of material quality.

In our previous works [12], [13], we demonstrated a novel SAG technique for the fabrication of multi-wavelength DFB laser arrays. By SAG of only the upper separate confinement heterostructure (SCH) layer of the DFB lasers, laser arrays with highly uniform wavelength spacing can be obtained [12]. Our SAG technique needs a simple process and is fitful for mass production of laser arrays. In this work, we show that the SAG technique can be conveniently used in combination with the bundle integrated guide (BIG) technique [14], [15] for the fabrication of combiner integrated with laser arrays. The power loss of light between the passive waveguide fabricated by the BIG technique is known to be extremely low [15]. A prototype four wavelength DFB laser array with multimode interference (MMI) coupler as combiner is fabricated. Because the process of our SAG technique is inherently compatible with that of the BIG technique, only a simple fabrication procedure is needed for the integrated device. The results presented in this paper indicate that cost-effective high-performance OLT light sources can be obtained with our method.

2. Experimental Procedure

A top-view optical microscope image of the fabricated device is shown in Fig. 1. The device consists of three sections: a DFB laser array section, an MMI combiner section, and a semiconductor optical amplifier (SOA) section. The separation between two laser elements is 250 μm. The laser elements of the array are connected with the MMI combiner with s-bend waveguides. A three-step metal–organic chemical vapor deposition (MOCVD) process is needed for the

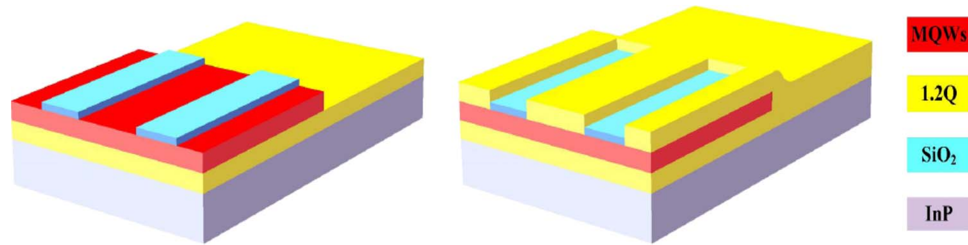

Fig. 2. Schematic structures of the wafer during the fabrication process.

fabrication of the device. In the first MOCVD step, a 1000-nm n-doped InP buffer layer, a 100-nm InGaAsP lower SCH layer lattice matched to InP ($\lambda_{PL} = 1.2$ μm, PL stands for photoluminescence), a 20-nm InP etch stop layer, and an MQW layer are first grown on the substrates. The MQW layer consists of 6 compressively strained InGaAsP wells ($+1.1 \times 10^{-2}$, $\lambda_{PL} = 1.59$ μm) and 7 tensile-strained InGaAsP layers (-3×10^{-3}, $\lambda_{PL} = 1.2$ μm). Then, SiO_2 mask strip pairs with gradually changed dimensions for different laser elements are formed on the MQW layer in only the laser areas of the wafer. The MQW layer and the etch stop layer in the passive waveguide regions are then selectively removed by wet etching using $H_2SO_4 : H_2O_2 : H_2O = 3 : 1 : 1$ solution and $H_2O : HCl = 4 : 1$ solution, respectively. The schematic structure of the wafer is shown in Fig. 2(a). In the second MOCVD step, an un-doped, p-doped, and n-doped InGaAsP layer lattice matched to InP ($\lambda_{PL} = 1.2$ μm) are successively grown on the patterned wafer and have thicknesses of 100 nm, 5 nm, and 7 nm, respectively, on plane substrates. The schematic structure of the obtained wafer is shown in Fig. 2(b). The p- and n-doped InGaAsP layers form a reverse junction, inducing a weak gain coupling into the grating structure and helping to increase the rate of single-mode lasing [12]. Gratings with uniform pitches are then formed in the InGaAsP layers by conventional holographic exposure combined with conventional photolithography. The p- and n-doped InGaAsP layers in other than the laser areas are etched away during the dry etching process for forming the gratings.

In the laser areas of the wafer, the InGaAsP layers grown in the second MOCVD step is the upper SCH layer of the DFB lasers and only the thickness of the layer is modulated by the SiO_2 patterns to get different emission wavelengths. Unlike the conventional MQW SAG technique, the optical properties of the MQW layer, which are sensitive to different growth conditions, are not affected, resulting in a precise control of wavelength spacing of the fabricated laser arrays [13]. Except for the SiO_2 patterns, the above process is the same as that of the BIG process [14], [15]. In the passive waveguide regions, both the InGaAsP layer grown in the first MOCVD step and the layers in the second MOCVD step form the core layer of the passive waveguides with a total thickness of more than 200 nm. The 1.2-μm emission wavelength of the InGaAsP layers is far away from the laser wavelength, resulting in a very low absorption loss. An SEM image of the cross-section of the interface between the laser and the passive waveguide is shown in Fig. 3. As can be seen, the surface of the joint portion is flat, making the MOCVD process easy to be conducted and repeatable. With the BIG scheme, an up to 99% coupling efficiency between the passive and active waveguides can be expected [15]. Unlike the offset waveguide structure [7], the decrease of optical confinement of the active MQW layer resulting from the integration of the passive layer is negligibly small. It is obvious that the SAG process is inherently compatible with the BIG process. In a single epitaxial process, both multiwavelength emissions with uniform spacing and high-quality passive waveguide material can be realized, which greatly helps in simplifying the fabrication procedure of the integrated device, noticeably reducing the cost of the device. A 1500 nm p-doped InP cladding layer and a 300 nm p^+-doped InGaAs contact layer are grown in the third MOCVD step finishing the material growth of the device.

While a shallow ridge waveguide is adopted for the DFB lasers and the SOA, the passive waveguides have a deep ridge structure. To realize the different structures, two separate

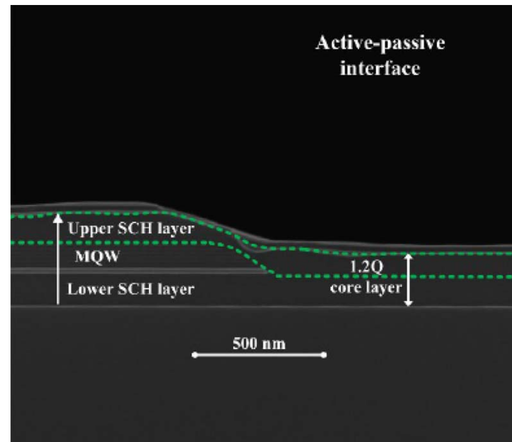

Fig. 3. SEM images of the cross section of the interface between the laser and the passive waveguide.

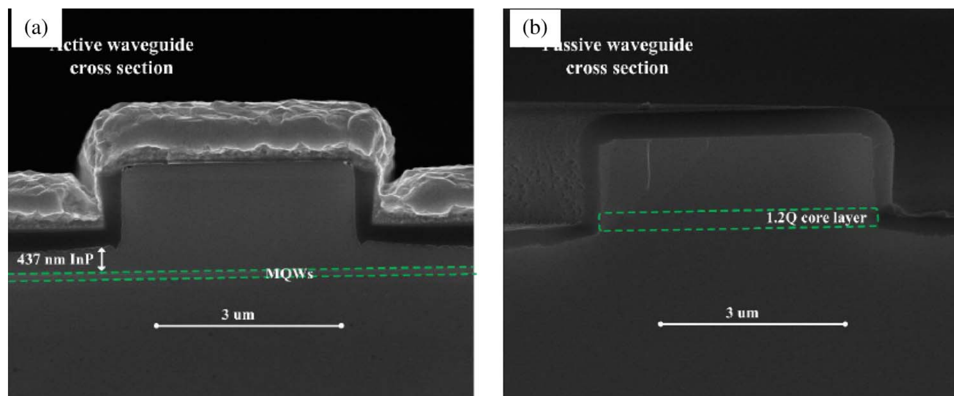

Fig. 4. SEM images of the cross section of the (a) active waveguide and the (b) passive waveguide.

etching steps, i.e., a wet etching step and a dry etching step, are usually needed [16]. To further simplify the fabrication of our device, we propose a new procedure as follows. The InGaAs contact layer in the passive regions of the wafer is first selectively etched away by $H_2SO_4 : H_2O_2 : H_2O = 3 : 1 : 1$ solution. SiO_2 masks are formed covering the areas of the ridges of the lasers, the SOA, and the passive waveguides. Inductively Coupled Plasma (ICP) etching is then conducted using a Cl_2, CH_4, and Ar gas mixture. The etching rate of the InGaAs contact layer during the RIE process is found to be slower than the etching rate of the InP and InGaAsP material, which are about 0.27, 0.67, and 0.54 μm/min, respectively. Thus, by controlling the duration of the dry etching process, the shallow ridge structure of the DFB lasers and the SOA and the deep ridge structure of the passive waveguides can be obtained by a single dry etching step, helping to ease the fabrication process noticeably. The widths of the laser waveguide, the s-band, and the output and the input waveguides of the MMI coupler are all 3 μm. The length and width of the MMI coupler are 320 and 24 μm, respectively. Fig. 4(a) and (b) shows the cross-section SEM images of the laser waveguide and the passive waveguide of a fabricated device. Ti/Au and Au/Ge/Ni are used as p- and n-electrode, respectively. The device is mounted onto a Cu heat sink and characterized at room temperature. The optical output power of the device is measured by an integrating sphere. For wavelength characterization, the light from the device is coupled into a single mode fiber and measured by an optical spectrum analyzer (OSA).

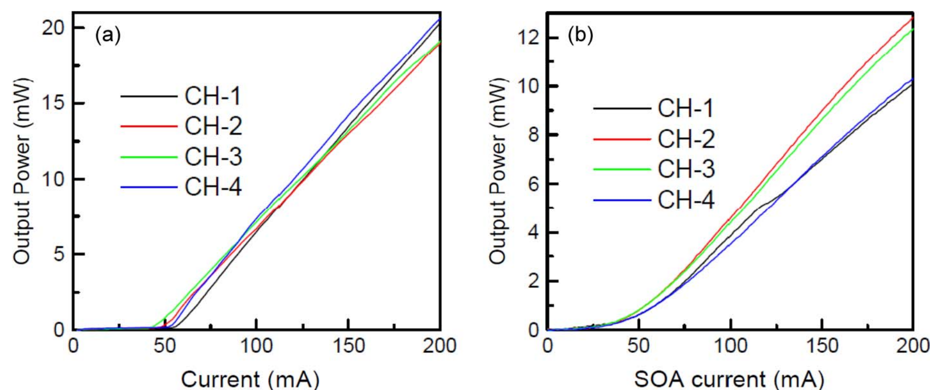

Fig. 5. (a) L–I characteristics measured from the laser end. (b) Output power as a function of SOA current when the DFB current is 100 mA.

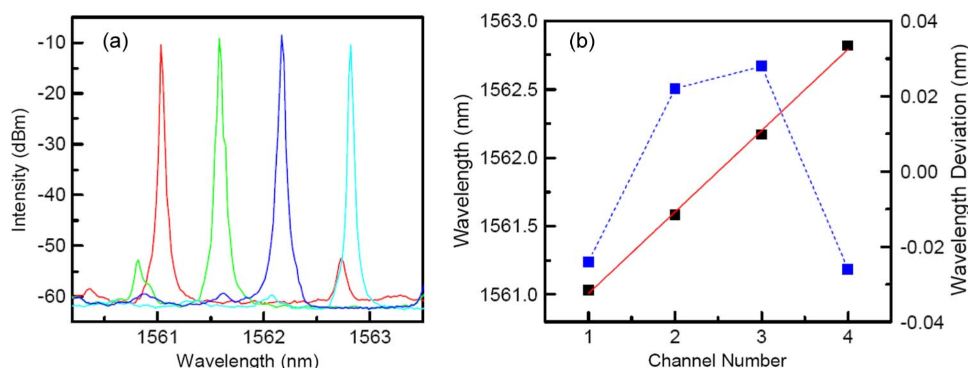

Fig. 6. (a) Optical spectra and (b) wavelengths and wavelength deviations of the lasers in the array.

3. Device Characterizations and Discussions

The light output versus current (L–I) characteristics of a fabricated device measured from the laser end are shown in Fig. 5(a). The threshold currents of the lasers are around 50 mA, which is apparently larger than the threshold currents of the DFB laser arrays fabricated with the upper SCH SAG technique [12]. The large threshold currents of this prototype integrated device are attributed to the unoptimized dry etching conditions of the waveguides. As can be seen from Fig. 4(a), while the etching time is enough for the formation of the deep ridge structure of the passive waveguides, there are an over 400 nm InP layer left on both sides of the ridge of the DFB laser, which leads to a serious lateral current diffusion. For each laser element in the array, about 17 mW light power can be obtained at 200 mA inject current, with a 0.11 W/A slope efficiency. Both the threshold current and the slope efficiency can be improved by optimizing the time of the dry etching process. The coupling loss between the active waveguides and the passive waveguides fabricated by the BIG technique is very small [14], [15]. There are, however, optical losses from the free carrier absorption in the p-doped cladding and the inherent insertion loss for the MMI coupler. Without the SOA the light power collected in the output waveguide of the MMI coupler is less than 2 mW for a single wavelength at 200 mA inject current. With the SOA the light output of the lasers can be boosted effectively. As shown in Fig. 5(b), the laser power can be enlarged to be over 10 mW at 20 °C, with currents of 200 mA and 100 mA for the SOA and DFB sections, respectively. A larger output power of OLT light sources helps to improve the power budget and the scalability of the WDM-PONs and thus is highly desirable.

The optical spectra of the lasers in the array are shown in Fig. 6(a). All the spectra were obtained at an inject current of 180 mA. As can be seen, the side mode suppression ratios

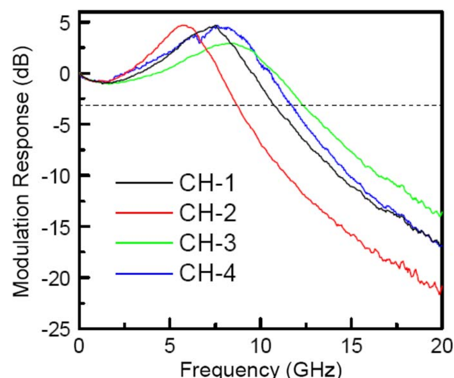

Fig. 7. Electrical to optical response of the laser elements. The bias current of the lasers is 100 mA.

(SMSRs) of all the laser elements are larger than 42 dB. The emissions of the laser array have an average spacing of 0.6 nm. The wavelengths for the different channels show very good linearity as can be seen from Fig. 6(b). The wavelength deviations with respect to the corresponding linear fitting values are between -0.03 nm and $+0.03$ nm. As shown in our previous works [12], [13], with our upper SCH SAG method, the thickness of only the upper SCH layer of the lasers is varied to realize different emission wavelengths. Contrary to the conventional MQW SAG process, the laser elements of the fabricated arrays have the same high-quality lower SCH and MQW material. Accompanied by the ability of the MOCVD system to control the thickness and composition of material with high accuracy, laser arrays with highly uniform wavelength spacing can thus be fabricated. What is more important, the SAG process is very simple and, thus, fits the mass production of low-cost laser arrays. By using the partially gain-coupled grating structure as in our device, a high single-mode yield, which is another important factor for the fabrication of multi-wavelength laser arrays, can also be realized [13].

The fabrication of laser arrays by using the upper SCH SAG technique combined with the BIG technique also has a high flexibility of device design. In the device presented in this paper, the thickness of the waveguide core layer is 200 nm. To confine the optical power better in the waveguide and thus reduce the transmission loss, a thicker core layer is helpful. This can be achieved by simply increasing the thickness of both the upper and lower SCH layer thickness of the lasers. The desired wavelength spacing of the laser array can be maintained by changing the varying step of the SiO_2 mask for the SAG process. For example, with the same mask pattern, a thicker upper SAG layer leads to a larger thickness difference between two nearby lasers and thus a larger wavelength difference. To get the needed spacing, a smaller increase step of the SiO_2 mask can be used.

The small signal direct modulation properties of the fabricated device are measured with a 50-GHz network analyzer. The obtained electrical to optical response of the laser elements is shown in Fig. 7. The measured 3-dB frequency bandwidths are larger than 9 GHz, which is enough for 10 Gb/s modulation. To extend the reach distance of the PONs, electro-absorption modulator (EAM) can be used because the chromatic dispersion effect is weaker for EAMs than direct modulation lasers. With the scheme presented above, EAM can be integrated into the device when the so-called identical active layer technique is used [17]. By properly setting the pitch of the gratings, the center wavelength of the laser array can be tuned to be several tens of nanometers larger than the gain peak of the MQW material. EAM function can thus be realized without any additional fabrication steps. In our prototype device, the SOA is placed after the MMI combiner, which is proper when the device is used as a tunable light source [18]. However, when all the channels are modulated at the same time as in the OLTs in WDM-PONs, the SOA will introduce optical crosstalk by the cross-gain modulation (XGM) effect. The effect may be alleviated by approaches such as the feed-forward technique [19] or can be eliminated by placing the SOA before the combiner. The present device shows that the integration

of SOAs is compatible with the proposed scheme for the fabrication of monolithic OLT light sources.

4. Conclusion

To summarize, a method for the fabrication of high-quality multi-wavelength DFB laser array monolithically integrated with a passive optical combiner is presented. By combining the upper SCH SAG technique and the BIG technique, both multi-wavelength emission with highly uniform spacing and low-loss passive waveguide material can be obtained in a single MOCVD growth step. A prototype laser array having four DFB laser elements and an MMI coupler as combiner is successfully fabricated. Only a very simple fabrication procedure is need, which greatly helps in reducing the cost of the device. It is also shown that with the method, EAM can also be easily integrated into the device. Our method is promising for the fabrication of cost-effective OLT light sources for WDM-PONs.

References

[1] R. P. Davey *et al.*, "Long-reach passive optical networks," *J. Lightw. Technol.*, vol. 27, no. 3, pp. 273–291, Feb. 2009.
[2] F. Ponzini *et al.*, "Evolution scenario toward WDM-PON [Invited]," *J. Opt. Commun. Netw.*, vol. 1, no. 4, pp. C25–C34, Sep. 2009.
[3] S. Y. Kim, S. B. Jun, Y. Takushima, E. S. Son, and Y. C. Chung, "Enhanced performance of RSOA-based WDM PON by using Manchester coding," *J. Opt. Netw.*, vol. 6, no. 6, pp. 624–630, Jun. 2007.
[4] C. Su, Y. C. Chi, H. Y. Chen, and G. R. Lin, "Using self-feedback controlled colorless Fabry–Perot laser diode for remote control free single-mode DWDM-PON transmission," *IEEE J. Quantum Electron.*, vol. 50, no. 8, pp. 658–668, Aug. 2014.
[5] L. Han *et al.*, "Electroabsorption-modulated widely tunable DBR laser transmitter for WDM-PONs," *Opt Exp.*, vol. 22, no. 24, pp. 30 368–30 376, Dec. 2014.
[6] S. H. Oh *et al.*, "200 GHz-spacing 8-channel multi-wavelength lasers for WDM-PON optical line terminal sources," *Opt. Exp.*, vol. 17, no. 11, pp. 9401–9407, May 2009.
[7] Z. Chung-En *et al.*, "Multiwavelength DFB laser arrays with integrated combiner and optical amplifier for WDM optical networks," *IEEE J. Sel. Topics Quantum Electron.*, vol. 3, no. 2, pp. 584–597, Apr. 1997.
[8] C. Zhang *et al.*, "Multi-channel DFB laser arrays fabricated by SAG technology," *Opt. Commun.*, vol. 300, pp. 230–235, Jul. 2013.
[9] G. P. Li, T. Makino, A. Sarangan, and W. Huang, "16-Wavelength gain-coupled DFB laser array with fine tunability," *IEEE Photon. Technol. Lett.*, vol. 8, no. 1, pp. 22–24, Jan. 1996.
[10] C. Zhang *et al.*, "The fabrication of 10-channel DFB laser array by SAG technology," *Opt. Commun.*, vol. 311, pp. 6–10, Aug. 2013.
[11] S. C. Nicholes *et al.*, "An 8 $\times$ 8 InP monolithic tunable optical router (MOTOR) packet forwarding chip," *J. Lightw. Technol.*, vol. 28, no. 4, pp. 641–650, Feb. 2010.
[12] C. Zhang, S. Liang, H. Zhu, B. Wang, and W. Wang, "A modified SAG technique for the fabrication of DWDM DFB laser arrays with highly uniform wavelength spacings," *Opt. Exp.*, vol. 20, no. 28, pp. 29 620–29 625, Dec. 2012.
[13] C. Zhang, S. Liang, H. Zhu, L. Han, and W. Wang, "Multichannel DFB laser arrays fabricated by upper SCH layer SAG technique," *IEEE J. Quantum Electron.*, vol. 50, no. 2, pp. 92–97, Feb. 2014.
[14] Y. Tohmori, K. Komori, S. Arai, and Y. Suematsu, "Low-threshold-current CW operation of 1.5 μm GaInAsP/InP bundle-integrated-guide distributed-Bragg-reflector (BIG-DBR) lasers," *Electron. Lett.*, vol. 21, no. 17, pp. 743–745, Aug. 1985.
[15] Y. Tohmori, X. Jiang, S. Arai, F. Koyama, and Y. Suematsu, "Novel structure GaInAsP/InP 1.5–1.6 μm bundle integrated-guide (BIG) distributed Bragg reflector laser," *Jap. J. Appl. Phys.*, vol. 24, no. 6, pp. L399–L401, Jun. 1985.
[16] S. Kanazawa *et al.*, "A compact EADFB laser array module for a future 100-Gb/s Ethernet transceiver," *IEEE J. Sel. Topics Quantum Electron.*, vol. 17, no. 5, pp. 1191–1197, Sep./Oct. 2011.
[17] C. Z. Sun *et al.*, "Fabrication and packaging of 40-Gb/s AlGaInAs multiple-quantum-well electroabsorption modulated lasers based on identical epitaxial layer scheme," *J. Lightw. Technol.*, vol. 26, no. 9–12, pp. 1464–1471, May/Jun. 2008.
[18] H. Ishii *et al.*, "Widely wavelength-tunable DFB laser array integrated with funnel combiner," *IEEE J. Sel. Topics Quantum Electron.*, vol. 13, no. 5, pp. 1089–1094, Sep./Oct. 2007.
[19] C. R. Doerr, C. H. Joyner, M. Zirngibl, L. W. Stulz, and H. M. Preby, "Elimination of signal distortion and crosstalk from carrier density changes in the shared semiconductor amplifier of multifrequency signal sources," *IEEE Photon. Technol. Lett.*, vol. 7, no. 10, pp. 1131–1133, Oct. 1995.